Human Molecular Genetics, 2016, Vol. 25, No. 24 5395–5406

doi: 10.1093/hmg/ddw356
Advance Access Publication Date: 24 October 2016
Original Article

ORIGINAL ARTICLE

High levels of sarcospan are well tolerated and act as a sarcolemmal stabilizer to address skeletal muscle and pulmonary dysfunction in DMD

Elizabeth M. Gibbs[1,2], Jamie L. Marshall[1,2,†], Eva Ma[1,2], Thien M. Nguyen[1,2], Grace Hong[1,2], Jessica S. Lam[1,2], Melissa J. Spencer[2,4] and Rachelle H. Crosbie-Watson[1,2,3,4,*]

[1]Department of Integrative Biology and Physiology, [2]Center for Duchenne Muscular Dystrophy, [3]Department of Neurology David Geffen School of Medicine and [4]Molecular Biology Institute, University of California Los Angeles CA 90095, USA

*To whom correspondence should be addressed at: Rachelle H. Crosbie-Watson, Department of Integrative Biology and Physiology, Department of Neurology, University of California Los Angeles, 610 Charles E. Young Drive East, Terasaki Life Sciences Building, Los Angeles, CA 90095, USA. Tel: 310 794 2103; Fax: 310 206 3987; Email: rcrosbie@physci.ucla.edu

Abstract

Duchenne muscular dystrophy (DMD) is a genetic disorder that causes progressive muscle weakness, ultimately leading to early mortality in affected teenagers and young adults. Previous work from our lab has shown that a small transmembrane protein called sarcospan (SSPN) can enhance the recruitment of adhesion complex proteins to the cell surface. When human SSPN is expressed at three-fold levels in *mdx* mice, this increase in adhesion complex abundance improves muscle membrane stability, preventing many of the histopathological changes associated with DMD. However, expressing higher levels of human SSPN (ten-fold transgenic expression) causes a severe degenerative muscle phenotype in wild-type mice. Since SSPN-mediated stabilization of the sarcolemma represents a promising therapeutic strategy in DMD, it is important to determine whether SSPN can be introduced at high levels without toxicity. Here, we show that mouse SSPN (mSSPN) can be overexpressed at 30-fold levels in wild-type mice with no deleterious effects. In *mdx* mice, mSSPN overexpression improves dystrophic pathology and sarcolemmal stability. We show that these mice exhibit increased resistance to eccentric contraction-induced damage and reduced fatigue following exercise. mSSPN overexpression improved pulmonary function and reduced dystrophic histopathology in the diaphragm. Together, these results demonstrate that SSPN overexpression is well tolerated in *mdx* mice and improves sarcolemma defects that underlie skeletal muscle and pulmonary dysfunction in DMD.

Introduction

Duchenne muscular dystrophy (DMD) is caused by mutations in the *DMD* gene, resulting in loss of the dystrophin protein and its associated protein complex, the dystrophin-glycoprotein complex (DGC) (1–3). The DGC acts as a link between the

[†]Current address: Broad Institute of MIT and Harvard, Cambridge 02142, MA, USA.
Received: June 27, 2016. **Revised:** September 26, 2016. **Accepted:** October 13, 2016

intracellular cytoskeleton and the surrounding extracellular matrix, providing structural stability to the sarcolemma during muscle contraction (4–6). Although additional protein complexes provide some compensatory adhesion to the extracellular matrix, the sarcolemma is susceptible to contraction-induced damage in the absence of dystrophin and the DGC (7,8). Over time, the progressive loss of membrane integrity leads to cycles of muscle fibre degeneration/regeneration and ultimately leads to muscle cell death.

In addition to the DGC, two other major adhesion complexes are found at the muscle cell surface: the utrophin-glycoprotein complex (UGC) and the α7β1 integrin complex (9–11). Utrophin is a ubiquitously expressed gene that shares close homology to dystrophin, and the composition of the UGC is largely identical to the DGC (12,13). In non-dystrophic muscle, the UGC is largely restricted to the postsynaptic region of neuromuscular junctions. The α7β1 integrin complex provides additional linkage and signalling between the cytoskeleton and extracellular matrix (10,11). In DMD, the UGC and α7β1 integrin complexes partially compensate for the absence of dystrophin by stabilizing the sarcolemma during the mechanical stress of muscle contraction.

SSPN is a transmembrane protein localized to the sarcolemma and the smallest core component of both the DGC and UGC, and it also interacts with the α7β1 integrin complex (14–17). Previous work from our lab has shown that overexpression of SSPN increases the cell membrane localization of all three skeletal muscle adhesion complexes (18–20). This finding has particular importance in the context of DMD, because numerous studies have shown that the upregulation of compensatory adhesion complexes can reduce or eliminate many of the dystrophic changes that occur in the absence of dystrophin (21–25). Previous work from our laboratory has demonstrated that moderate overexpression of human SSPN in the *mdx* mouse model of DMD increases membrane expression of the UGC and α7β1 integrin complex, reducing markers of dystrophic pathology and increasing membrane stability (18,19). These findings suggest that SSPN serves as a key determinant in the expression level of adhesion complexes at the sarcolemma, and that this role could be leveraged as a therapeutic target in DMD.

We have previously shown that approximately three-fold overexpression of human SSPN (hSSPN) can rescue aspects of the *mdx* phenotype by increasing expression of utrophin and associated proteins throughout the extrasynaptic sarcolemma (18,19,26). At levels of approximately 0.5 or 1.5 fold expression, hSSPN was not able to ameliorate *mdx* pathology, suggesting that a minimum three-fold level overexpression of SSPN is necessary for rescue (19). However, expressing higher levels of hSSPN in wild-type mice (ten-fold transgenic expression) caused a severe degenerative muscle phenotype that led to premature death (27). Biochemical evidence suggests that human-specific and mouse-specific SSPN proteins in hSSPN-Tg muscle form insoluble aggregates of SG-SSPN complexes. This aggregation destabilizes the stability of α-DG within the DGC binding to laminin, and leads to disorganization of the extracellular matrix. It remains unclear whether the toxicity observed in hSSPN transgenic mice is inherent to SSPN overexpression, or if it is specific to aberrant interactions between hSSPN and endogenous mouse SSPN.

Because we are pursuing genetic and pharmacological upregulation of SSPN as a therapeutic avenue, it is imperative to determine whether there is an upper limit of SSPN overexpression to address concerns related to toxicity. Furthermore, the ability of SSPN to affect skeletal and pulmonary functions has not been reported. To directly address these questions, we generated four lines of mice expressing multiple levels of mSSPN. In the present study, we show that 30-fold overexpression of mSSPN does not cause deleterious effects in muscle, and leads to a histologic improvement in *mdx* mouse muscle that is similar to the beneficial effect of low levels of hSSPN. We demonstrate that mSSPN overexpression reduces membrane fragility in *mdx* skeletal muscle and improves muscle function in several different outcome measures. Pulmonary function is improved in *mdx*:mSSPN-Tg mice and the severe dystrophy associated with the *mdx* diaphragm is ameliorated. These findings reveal that high levels of SSPN overexpression in muscle are not only well tolerated, but significantly strengthen skeletal and respiratory parameters. Taken together, these data support the pursuit of SSPN as a potential therapeutic target in this disease. We are particularly encouraged that SSPN has broad applicability as an additive treatment that is expected to boost the efficacy of all therapies that are currently in clinical testing.

Results

mSSPN increases adhesion complexes at the sarcolemma

We generated mSSPN transgenic mice expressing full-length mSSPN cDNA under control of the human skeletal α-actin promoter (Supplementary Material, Fig. S1A). Four independent founder lines of mSSPN-Tg mice (lines 28, 32, 23 and 15; Supplementary Material, Fig. S1B) were analysed for mSSPN transgene expression, and the highest expressing line was chosen for detailed analysis. Based on immunoblot analysis, this line expresses mSSPN at approximately 30-fold over endogenous levels, as determined by immunoblot (line 28; Supplementary Material, Fig. S1C). Previous work from our lab has shown that ten-fold transgenic expression of human SSPN in wild-type mice leads to a severe muscle phenotype that includes muscle degeneration, kyphosis and death at 6-10 weeks of age (27). By contrast, wild-type mice overexpressing mSSPN are healthy, breed well, exhibit no signs of muscle pathology, and appear to have a normal lifespan (the oldest transgenic carriers in our colony are currently over 2.5 years of age).

Male mSSPN-Tg mice were crossed to *mdx* females to generate dystrophin-deficient mice expressing transgenic mSSPN (*mdx*:mSSPN-Tg). Robust expression of SSPN was detected at the sarcolemma of all transgenic wild-type (WT) and *mdx* mice (Fig. 1A and B, Supplementary Material, Fig. S1). Relative to WT muscle, WT:mSSPN-Tg had increased sarcolemmal localization of utrophin, dystrophin, and β1D integrin, showing that overexpression of mSSPN affects all three major adhesion complexes in muscle. Similarly, *mdx*:mSSPN-Tg showed increased levels of utrophin and β1D integrin at the sarcolemma. We additionally found increased abundance of the sarcoglycans in WT and *mdx* mice expressing mSSPN, although immunofluorescence did not reveal major changes in β-dystroglycan expression at the sarcolemma.

In order to specifically examine the abundance of adhesion complexes associated with the sarcolemma, muscle lysates were additionally assessed using sWGA lectin chromatography, which binds glycoproteins with GlcNAc glycans associated with the DGC and UGC (14). In this binding assay, protein interactions within complexes are preserved using a mild digitonin buffer followed by lectin binding, allowing analysis of intact adhesion complexes. By immunoblot of sWGA-enriched samples, we found that overexpression of mSSPN increased levels of DGC

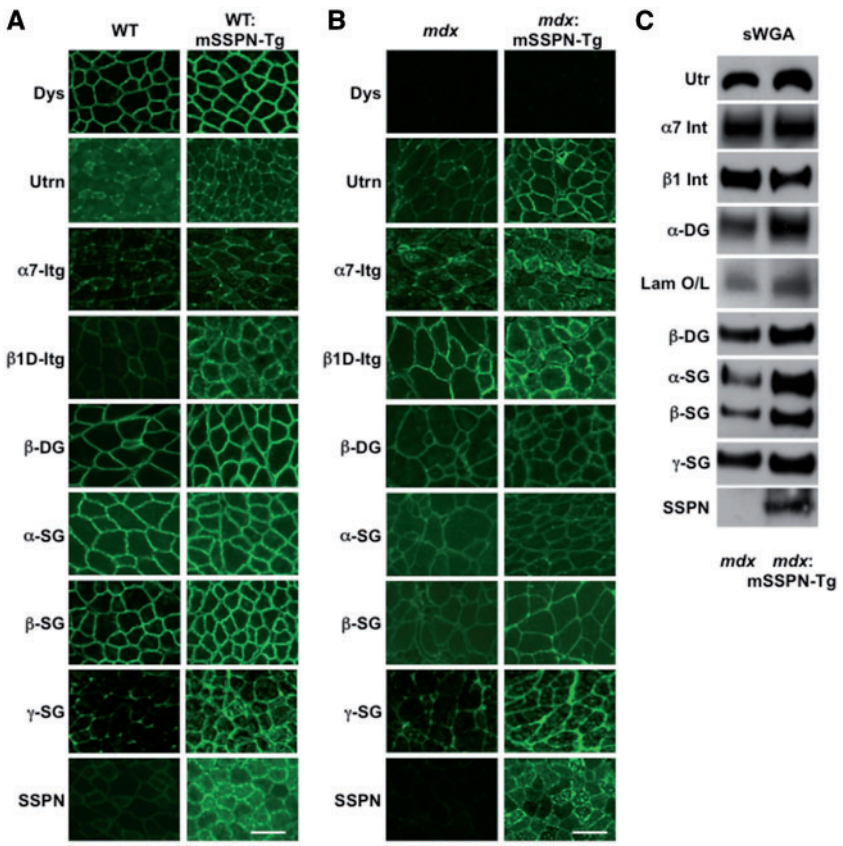

Figure 1. mSSPN can be highly expressed without toxicity and can restore some components of major muscle adhesion complexes. Transverse sections of WT, WT:mSSPN-Tg, (**A**) *mdx* and *mdx*:mSSPN-Tg (**B**) quadriceps were stained with antibodies against components of the three major muscle adhesion complexes. Bar, 100 μm. (**C**) Skeletal muscle lysates from *mdx* and *mdx*:mSSPN-Tg were solubilized using digitonin and enriched using sWGA lectin chromatography. Eluates were resolved by SDS–PAGE and immunoblotted with indicated antibodies. Laminin overlay onto α-DG is also shown (lam O/L).

and UGC components associated with the sarcolemma (Fig. 1C). Laminin binding to α-DG was additionally assessed by overlaying laminin protein onto sWGA-enriched skeletal muscle lysates, revealing an increase in *mdx*:mSSPN-Tg laminin binding.

Overexpression of mSSPN improves dystrophic pathology and membrane stability in *mdx* mice

We next examined *mdx*:mSSPN-Tg muscle for changes in the dystrophic pathology associated with the *mdx* phenotype. At 6 weeks, haematoxylin and eosin (H&E) stained transverse cryosections of quadriceps from *mdx*:mSSPN-Tg mice displayed a reduction of degeneration and necrosis relative to *mdx* littermates (Fig. 2A). Quantitative analysis of muscle cryosections also revealed a significant decrease in the percentage of fibres with central nuclei, indicating a reduction in the cycles of regeneration/degeneration that are normally associated with loss of dystrophin (Fig. 2A and B).

In DMD, the absence of dystrophin and subsequent loss of DGC-associated proteins at the sarcolemma leads to membrane instability and vulnerability to contraction-induced damage (7,8). To determine whether mSSPN expression decreases sarcolemmal disruption in *mdx* mice, we performed an *in vivo* tracer assay with Evans blue dye (EBD). EBD binds to albumin in blood serum, and accumulates in damaged and permeable muscle fibres (28). *mdx* mice displayed a high level of muscle fibres marked by EBD accumulation (Fig. 2C and D). Quads from *mdx*:mSSPN-Tg mice had significantly decreased EBD-positive fibres relative to *mdx* mice and were not significantly different from WT, demonstrating that mSSPN overexpression at levels as high as 30-fold improves sarcolemmal stability. To further examine the role of SSPN in stabilizing the sarcolemma, we tested serum creatine kinase (CK) levels in *mdx* mice, WT, and *mdx*:mSSPN-Tg mice at 6 months (Fig. 2E). Muscle damage and degeneration leads to elevated CK levels throughout the *mdx* lifespan. mSSPN-Tg overexpression significantly decreased serum creatine kinase levels relative to *mdx* mice, showing that mSSPN overexpression reduces sarcolemmal damage and leakage in *mdx* mice.

Transgenic mSSPN expression improves muscle strength and function in *mdx* mice

In order to investigate the effect of mSSPN transgene expression on muscle strength, forelimb grip strength was tested at 6 weeks (Fig. 3A). Grip strength provides a simple method to measure mouse forelimb strength *in vivo*. We performed five consecutive trials on each mouse five times, and found that *mdx* mice were significantly weaker by the fifth trial. In *mdx* mice overexpressing mSSPN, grip strength was significantly increased relative to *mdx* littermates.

During grip strength testing, we observed that *mdx*:mSSPN-Tg mice appeared more active than *mdx* littermates following the relatively mild exertion of the grip strength protocol. Based on

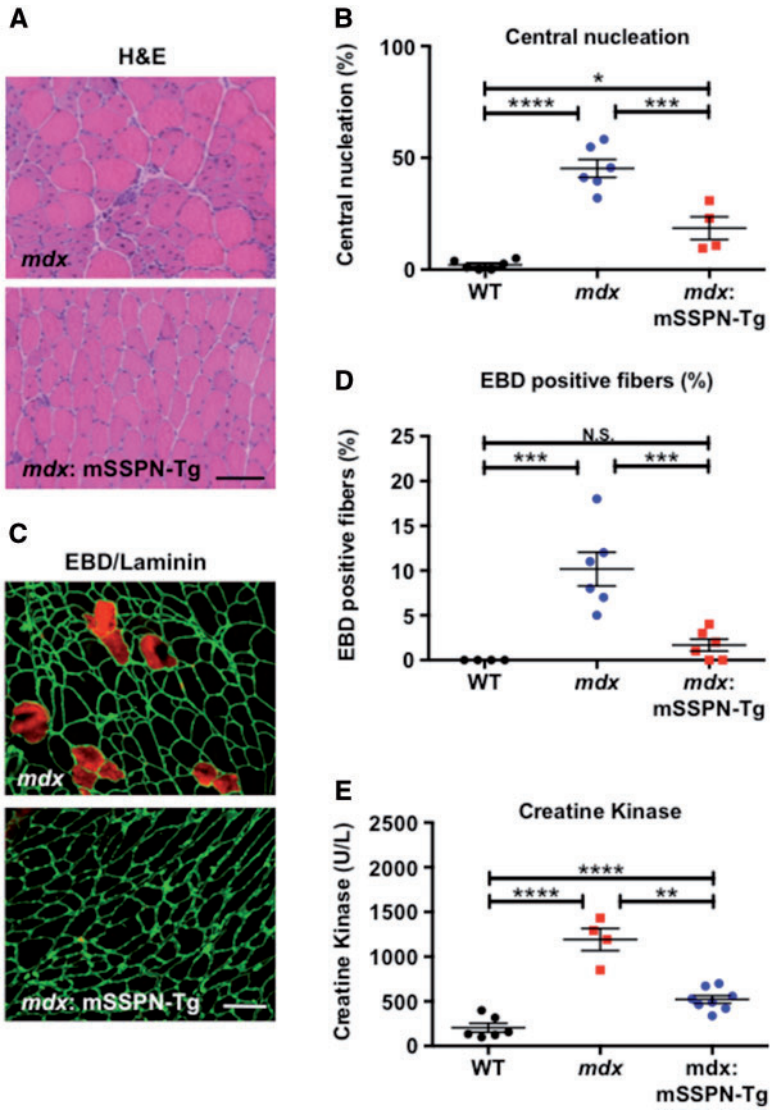

Figure 2. mSSPN overexpression greatly improves muscle histology and membrane stability in *mdx* mice. (**A**) Transverse sections of quadriceps muscle from 6 week old *mdx* and *mdx*:mSSPN-Tg mice were stained with H&E to visualize muscle pathology. Bar, 100 μm. (**B**) Sections from *mdx*:mSSPN-Tg quadriceps display reduced central nucleation relative to *mdx* muscle (WT, $n = 6$, *mdx* $n = 6$, *mdx*:mSSPN-Tg $n = 4$). (C&D) Quad sections from 6-week-old Evans Blue Dye (EBD)-injected *mdx*:mSSPN-Tg and *mdx* mice were stained with antibody against laminin (green) to delineate the sarcolemma. EBD-positive fibres were visualized by red fluorescence, which serves as a marker for membrane damage (WT $n = 4$, *mdx* $n = 6$, *mdx*:mSSPN-Tg $n = 6$). Bar, 100 μm. (E) Creatine kinase levels from serum were measured at 20 weeks of age (*mdx* $n = 4$, *mdx*:mSSPN-Tg $n = 8$, WT $= 6$). Data represent means ± SEM. Statistics calculated using one-way ANOVA followed by Tukey's multiple comparison's test (*$P < 0.05$, **$P < 0.01$, ***$P < 0.001$ and ****$P < 0.0001$).

this observation, we used an open field assay to test voluntary activity after exercise. Immediately following grip strength testing, 6-month-old mice were placed in a novel chamber and allowed to freely explore for 6 minutes. Animal activity was video recorded, and the position of the mouse was tracked over the testing period (Fig. 3B). While *mdx* mice moved very little during the 6 minutes following grip strength exercise, the voluntary activity of *mdx*:mSSPN-Tg littermates was significantly increased throughout the trial (Fig. 3C). Surprisingly, expression of the mSSPN transgene completely restored *mdx* activity to wild-type levels, as there was no significant difference between *mdx*:mSSPN-Tg and WT control activity post-exercise. When the mice were not challenged with a mild exercise protocol, there was no significant difference in distance travelled between WT, *mdx* and *mdx*:mSSPN-Tg mice (Supplementary Material, Fig. S2A and B).

Given the substantial improvement in mdx:mSSPN-Tg post-exercise activity, we tested nNOS levels in WT, *mdx* and *mdx*:mSSPN-Tg muscle to determine if mSSPN overexpression altered nNOS localization or abundance. nNOS is a component of the DGC and regulates vasorelaxation via the production of nitric oxide (29). In the absence of dystrophin, nNOS is lost from the sarcolemma and directly contributes to exercise-related fatigue in DMD (30,31). Although the mSSPN transgene restored post-exercise activity in *mdx*, we did not see any restoration of nNOS to the sarcolemma or increase in overall nNOS abundance (Supplementary Material, Fig. S2C and D).

Muscle physiology was tested on extensor digitorum longus (EDL) muscles isolated from WT, *mdx* and *mdx*:mSSPN-Tg mice at 5 months of age. EDL from *mdx* had a 25% decrease in specific force production relative to WT EDL (Fig. 3D). Overexpression of

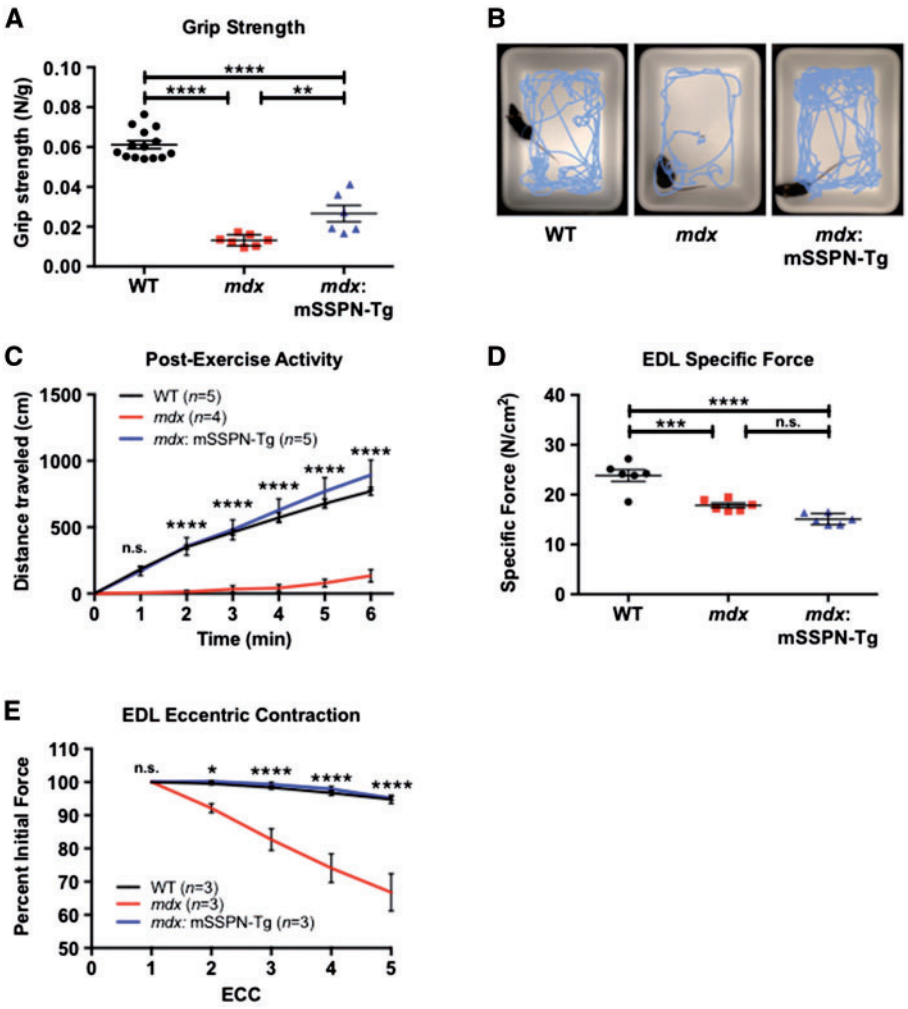

Figure 3. Transgenic expression of mSSPN improves muscle physiology in *mdx* mice. (**A**) Forelimb grip strength normalized to body weight at 6 weeks of age (fifth consecutive trial reported). (**B**) Representative traces of mouse activity in an open field during a 6 minute recording time. (**C**) Post-exercise walking distances at 6 months of age were recorded using an open field activity chamber (n=4 for *mdx*, n=5 for *mdx*:mSSPN-Tg and WT). (**D**) Specific force measurement in transgenic mice. (E) Force production in EDL as a percent of initial force, following a series of eccentric contractions (n=6 for all groups). Data represent means ± *SEM*. Statistics calculated using one-way ANOVA followed by Tukey's multiple comparison's test (A,D) or two-way ANOVA (C,E) (*$P < 0.05$, **$P < 0.01$ and ****$P < 0.0001$).

mSSPN did not improve specific force production, as there was no significant difference between *mdx* and *mdx*:mSSPN-Tg EDL (Fig. 3D). However, *mdx*:mSSPN-Tg EDL showed marked resistance to a series of eccentric contractions when compared to *mdx* EDL. While repeated eccentric contractions resulted in a large loss of force in the isolated *mdx* muscle, *mdx*:mSSPN-Tg muscle maintained a force output similar to WT during the protocol (Fig. 3E).

Expression of mSSPN reduces dystrophy in *mdx* diaphragm

As with other mouse models of muscular dystrophy, *mdx* mice have unusually thickened diaphragms at an early age (32–34). Upon dissection, we noted that diaphragms from *mdx*:mSSPN-Tg mice appeared thinner and less fibrotic than those of *mdx* littermates. In order to quantify this thickness relative to WT diaphragms, sections were taken from the anterolateral right costal muscle in WT, *mdx* and *mdx*:mSSPN-Tg mice at 6 weeks of age (Fig. 4A). We found that the expression of the mSSPN transgene reduced *mdx* diaphragm thickness to that of WT diaphragms (Fig. 4B). Similar to quadriceps, the number of fibres with centralized nuclei was also decreased in *mdx*:SSPN-Tg diaphragm (Fig. 4C and D). To determine whether mSSPN expression improves sarcolemmal stabilization in *mdx* diaphragm fibres, we additionally evaluated EBD uptake in the diaphragm (Fig. 4E and F). Diaphragms from 6-week-old *mdx*:mSSPN-Tg mice had a significant reduction in the number of positive EBD fibres relative to *mdx*, demonstrating that SSPN significantly reduces sarcolemmal susceptibility to injury.

SSPN improves pulmonary function in *mdx* mice

In most individuals with DMD, progressive weakness of respiratory muscles leads to pulmonary dysfunction and contributes to early mortality (35). In light of the changes seen in the *mdx*:SSPN-Tg diaphragm, a major respiratory muscle, we further assessed the effect of the mSSPN transgene on *mdx* pulmonary function. We found that mSSPN transgene expression was present in accessory respiratory muscles at levels comparable to limb muscle, and also expressed at lower levels in the heart (Fig. 5A). We monitored respiratory parameters in mice at 26

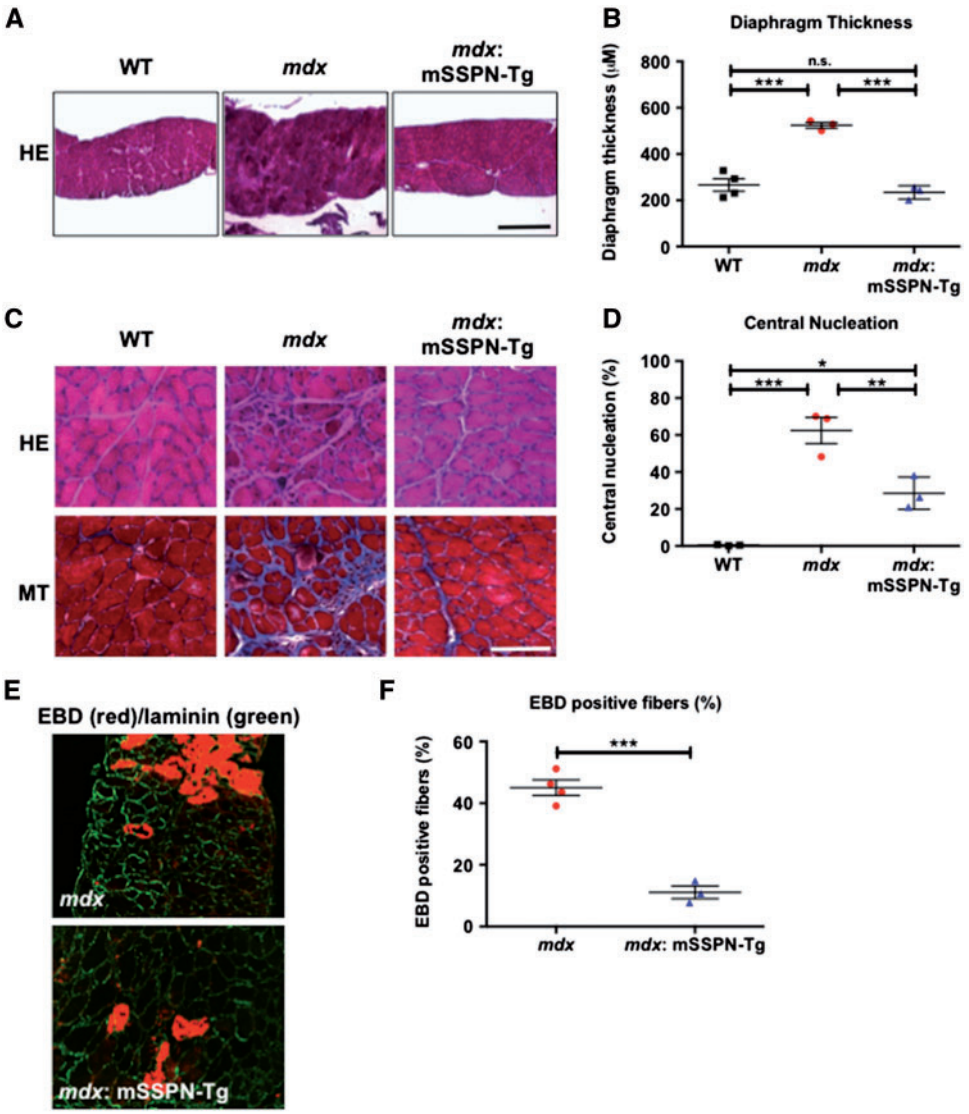

Figure 4. Diaphragms from *mdx*:mSSPN-Tg have reduced dystrophic pathology. (A&B) Transverse sections of diaphragm muscle from 6 week old *mdx* and *mdx*:mSSPN-Tg mice were stained with H&E to visualize muscle pathology. The average thickness of the diaphragm is shown (WT $n=4$, *mdx* $n=3$, *mdx*:mSSPN-Tg $n=3$, $P<0.0001$). Bar, 100 μm. (C&D) Sections were stained with H&E and Masson's trichrome (MT) to visualize muscle pathology. Bar, 200 μm. Fibres from *mdx*:mSSPN-Tg diaphragm exhibit reduced central nucleation ($n=3$ for all conditions). (E&F) Diaphragm sections from 6-week old Evans Blue Dye (EBD)-injected *mdx*:mSSPN-Tg show reduced EBD positive fibres compared with *mdx*, indicating an improvement in membrane stability. Statistics calculated using one-way ANOVA followed by Tukey's multiple comparison's test (B&D) or Student's *t*-test (**F**). Data represent means ± SEM. Statistics calculated using one-way ANOVA followed by Tukey's multiple comparison's test (**B**) or two-way ANOVA (D) (*$P < 0.05$, ***$P < 0.001$ and ****$P < 0.0001$).

weeks of age using whole-body plethysmography. Ventilation was measured at rest and during hypercapnic challenges as described by Capote and colleagues (36). None of the respiratory parameters tested were significantly different between WT and *mdx* mice during baseline room air conditions (Supplementary Material, Table S1). During the first hypercapnic challenge, measures of minute ventilation, respiratory frequency, peak inspiratory flow (PIF) and peak expiratory flow (PEF) were all significantly decreased in *mdx* mice relative to WT controls (Fig. 5A–D). Of these parameters, *mdx*:mSSPN-Tg mice showed significant improvements in minute ventilation and PEF relative to *mdx* mice (Fig. 5B and E), and no change in frequency or PIF (Fig. 5C and D).

In order to further evaluate the role of SSPN in maintaining respiratory muscle integrity, we assessed pulmonary function in mice lacking SSPN (SSPN-null). While lacking an overt dystrophic muscle phenotype at a young age (37), SSPN-null mice exhibit age-dependent skeletal and cardiac muscle pathology (16,26). No pulmonary deficits have previously been reported in this model. We tested the mice using whole-body plethysmography at 42 weeks of age at room air and during hypercapnic challenges. At baseline, minute ventilation, respiratory frequency and PIF were significantly decreased in SSPN-null mice relative to WT (Supplementary Material, Table S2). During the first hypercapnic challenge, both PIF and PEF were significantly decreased in SSPN-null mice relative to WT (Fig. 5F and G).

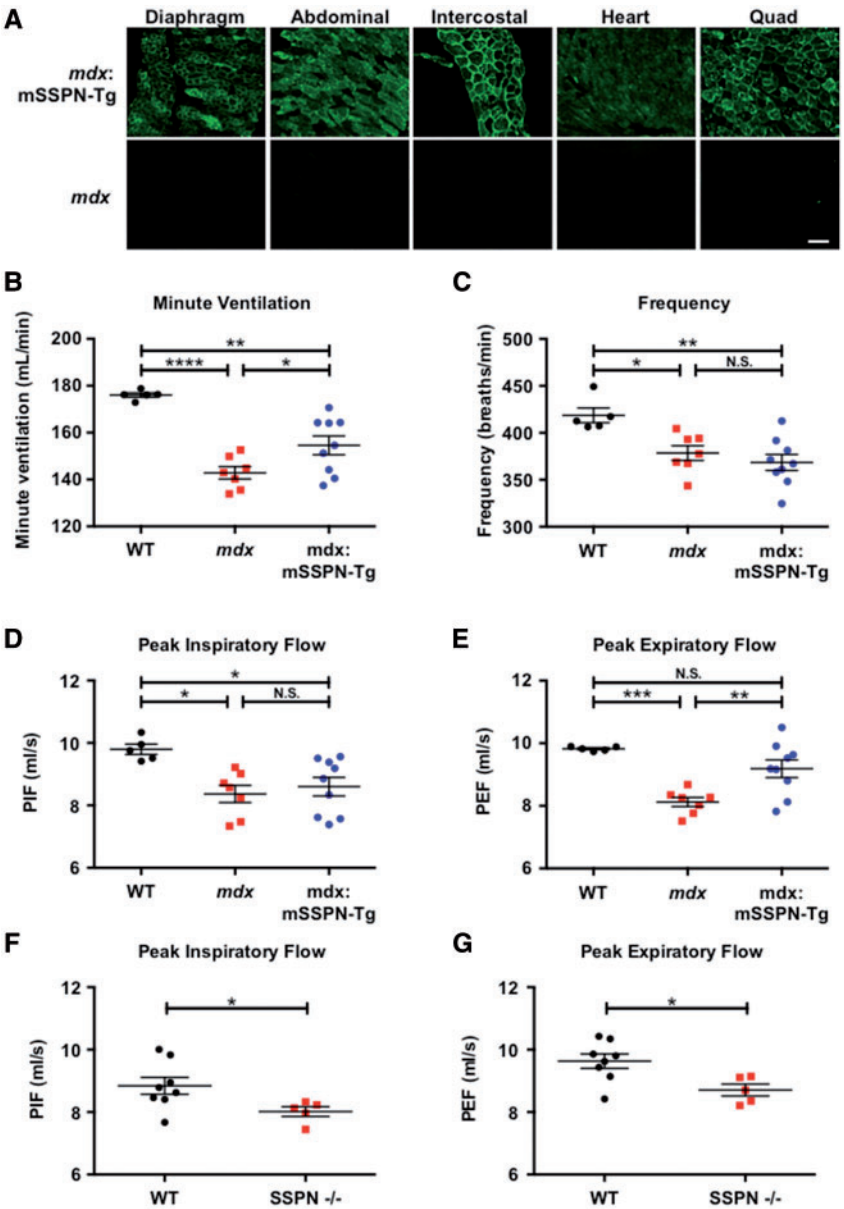

Figure 5. SSPN expression improves pulmonary function in *mdx* mice. (**A**) Transverse sections of the diaphragm, abdominal, intercostal and heart from were stained with antibody against SPPN in order to determine the relative SSPN expression in muscles associated with pulmonary function. Sections from quadriceps are shown for comparison. (**B–E**) The pulmonary function of age-matched WT, *mdx* and *mdx*:mSSPN-Tg mice was measured using whole-body plethysmography. Reported measurements were recorded during first hypercapnic challenge: minute ventilation (B), frequency (C), peak inspiratory flow (D), and peak expiratory flow (E). (**F,G**) To evaluate the effect of loss of SSPN on pulmonary function, age-matched WT and SSPN-null mice were also tested. Both peak inspiratory flow (F) and peak expiratory flow (G) were significantly decreased in SSPN-null mice. Data represent means ± *SEM*. Statistics calculated using one-way ANOVA followed by Tukey's multiple comparison's test (B-E) or Student's *t*-test (F-G) (*$P < 0.05$, **$P < 0.01$, ***$P < 0.001$ and ****$P < 0.0001$).

Interestingly, although PIF was decreased in SSPN-null mice, overexpression of mSSPN-Tg failed to rescue PIF in the *mdx* model, suggesting that dystrophin and sarcospan deficiencies cause distinct patterns of respiratory defects.

Discussion

Membrane damage is one of the earliest cellular events in the pathogenesis of DMD. In this study, we show that mSSPN overexpression reduces membrane damage in *mdx* mouse muscle, leading to overall reduced dystrophic pathology. These findings support the pursuit of SSPN upregulation as a therapeutic avenue for DMD and demonstrate that even very high levels of SSPN overexpression are not toxic in muscle. Similar to our previous studies of hSSPN overexpression in *mdx* and WT mouse muscle, our results show mSSPN increases localization of certain adhesion complex components at the sarcolemma. However, this increase is modest, suggesting that SSPN-mediated stabilization of the sarcolemma can occur through relatively low levels of adhesion complex upregulation. The

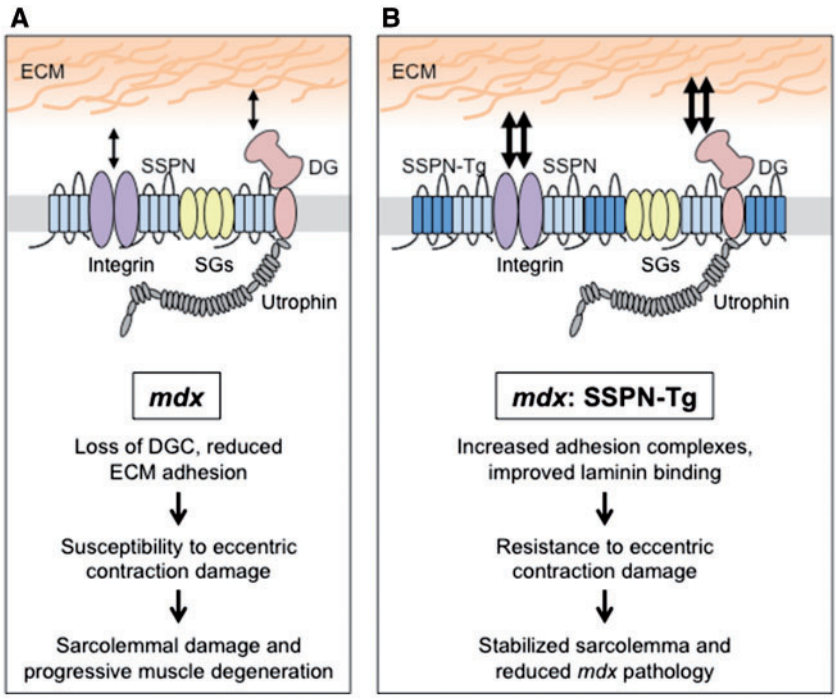

Figure 6. Schematic summarizing mSSPN transgenic overexpression in *mdx* muscle. The underlying deficit in DMD and related muscular dystrophies is the loss of protective connections between the sarcolemma and the extracellular matrix (ECM). Within the DGC and UGC, the dystroglycans link the membrane complex to laminin. In *mdx* muscle, the DGC is absent and leads to increased contraction-induced membrane damage. When mSSPN is overexpressed in *mdx* muscle, laminin binding is increased and sarcolemmal stability is enhanced. This increase in sarcolemmal stability leads to reduced muscle degeneration over time.

SSPN-mediated increase in adhesion complex localization leads to substantial improvement in the histopathological features of *mdx* muscle, consistent with previous studies from our laboratory. We additionally find that membrane stability, one of the earliest cellular events in the pathogenesis of DMD, is significantly ameliorated in *mdx* by the overexpression of mSSPN, as assessed by serum CK level and EBD tracer assay.

Here, we also show that SSPN overexpression ameliorates skeletal muscle some physiological deficits in *mdx* mice. Based on histological findings, we used several approaches to assess muscle function in *mdx*:mSSPN-Tg mice. While *in vitro* measurement of *mdx*:mSSPN-Tg EDL showed no improvement in force generation relative to *mdx*, the mSSPN transgene conferred substantial protection against eccentric contraction-induced damage. The susceptibility of *mdx* muscle to eccentric contraction is directly related to membrane integrity; force drop is thus viewed as an index of membrane fragility (38). Together with the improvements seen in the serum CK level and the EBD tracer assay, these findings demonstrate that SSPN overexpression has a substantial effect on membrane stability, and can help counter the progressive degeneration associated with dystrophin loss (Fig. 6A-B).

Previous studies have shown that voluntary activity in *mdx* mice is dramatically reduced following mild exercise protocols (30,39). During grip strength testing of *mdx* and *mdx*:mSSPN-Tg littermates, we noticed that while *mdx* mice appeared fatigued and lethargic immediately following testing, mice carrying the mSSPN transgene remained active and alert. When we formally tested this observation using an open field activity assay, we consistently found that *mdx*:mSSPN-Tg mice were as active as WT mice following the mild exertion of the grip strength protocol. This is particularly interesting in light of our grip strength findings: although *mdx*:mSSPN-Tg were able to exert approximately twice as much force in terms of repeated grip strength measures, the force was still far less than that of WT. Together with our *in vitro* data, these findings suggest that SSPN-mediated stabilization of the *mdx* sarcolemma ameliorates specific aspects of dystrophic physiology, and may improve fatigue-like properties while having minimal impact on overall muscle strength.

Diaphragm is one of the most affected muscles throughout the lifespan of the *mdx*, displaying a higher degree of fibrosis and fat infiltration than other skeletal muscles. We found that mSSPN overexpression substantially improves pathology of the diaphragm in *mdx* mice. Given that diaphragm is one of the major respiratory muscles, we evaluated pulmonary function in *mdx* and *mdx*:mSSPN-Tg mice. Previous studies have found varying degrees of change in *mdx* ventilation, but generally suggest that loss of dystrophin in mice leads to modest, age-dependent deficits in pulmonary function (33,40,41). In comparing *mdx* respiration to that of WT at approximately 6 months of age, we found that hypercapnic challenge induced significant changes in most respiratory parameters, although there was little difference during room air measurements. Expression of mSSPN improved several measurements in *mdx*, including MV and PEF. Surprisingly, PIF was not improved by mSSPN expression, although this measurement is thought to be particularly sensitive to diaphragm function. In order to better understand the role of SSPN in this highly active muscle, we additionally tested pulmonary function in WT and SSPN-null mice. Although loss of SSPN does not lead to a severe dystrophic muscle phenotype, we previously showed that the SSPN-null diaphragm is more vulnerable to eccentric contraction damage and generates reduced specific force (16). Consistent with these

findings, we found that both PIF and PEF are significantly decreased in SSPN-null mice relative to WT. These results are consistent with a key role for SSPN in maintaining sarcolemmal stability both in healthy and dystrophic muscle.

Our results, combined with previous findings from our laboratory, indicate that SSPN supports sarcolemmal stability in skeletal muscle through interaction with adhesion complexes. In the absence of dystrophin, this protective role prevents membrane damage and improves muscle physiology and pulmonary function. Many treatments currently in development for DMD are targeted at restoring the sarcolemmal connection to the extracellular matrix. The goal of these therapies is to increase membrane stability through either the direct replacement/restoration of dystrophin or the upregulation of other adhesion complex proteins. One major challenge in all of these potential treatments will be establishing enough protein at the cell membrane surface to produce a therapeutic effect (42). In light of these emerging therapies, identifying pathways that can enhance membrane localization of adhesion complexes and increase membrane stability is particularly important. SSPN is attractive as a potential therapeutic target, since it plays a direct role in stabilizing the sarcolemma, and additionally could serve to enhance localization of other adhesion complex proteins. This strategy is particularly appealing because it could also be used to augment other drug and gene therapies currently in development.

Materials and Methods

Animals

Wild-type (C57BL/6J) and *mdx* mice (C57Bl/10ScSn background) were purchased from Jackson Laboratories (Bar Harbor, ME, USA). SSPN-null mice were a generous gift from Dr. Kevin P. Campbell (University of Iowa Carver College of Medicine, Iowa City, IA) (37). Transgenic constructs were designed with the human skeletal actin promoter and VP1 intron upstream of the full-length mouse SSPN cDNA, as described previously (27,43). Transgenic mice were generated by microinjection of transgenic constructs into the pronucleus of fertilized single-cell embryos (C57BL/6J background, Transgenic Mouse Facility, University of California, Irvine), and four viable lines were recovered (Lines 28, 23, 32 and 15). Transgenic lines were maintained on a C57BL/6J background.

Males from each transgenic line were crossed to *mdx* females to generate transgenic *mdx* lines and maintained by sibling crosses (B6/B10ScSn background). Mice were maintained in the Terasaki Life Sciences Vivarium following guidelines established by the Institutional Animal Care and Use Committee at the University of California, Los Angeles (approval #2000-029-43) and approval for these studies was granted by the UCLA Animal Welfare Assurance (approval #A3196-01). All mice used in the study were male.

Skeletal muscle protein preparation

Prior to dissection, mice were euthanized using isoflurane. The total skeletal muscle was snap frozen in liquid nitrogen and stored at −80 °C. Tissues were ground to a fine powder using a liquid nitrogen-cooled mortar and pestle, added to ice-cold homogenization buffer and homogenized in radioimmunoprecipitation assay buffer (RIPA; Thermo Fisher Scientific) with protease inhibitors (0.6 μg/ml pepstatin A, 0.5 μg/ml aprotinin, 0.5 μg/ml leupeptin, 0.75 mM benzamidine, 0.2 mM PMSF, 5 μM calpain I, and 5 μM calpeptin). Homogenates were rotated at 4 °C for 1 h and clarified by centrifugation at 15,000 rpm for 20 min at 4 °C. Protein concentration was determined using the DC Protein Assay (Bio-Rad Laboratories), and lysates were stored at -80 °C.

sWGA enrichment

Sarcolemmal-associated α-DG complexes were enriched as previously described (16). Briefly, lysates from *mdx* and *mdx*:mSSPN-Tg was solubilized using 1% digitonin in homogenization buffer, and equal protein concentrations of clarified lysates were applied to succinylated wheat germ agglutinin (sWGA)-conjugated agarose beads (AL-1023S; Vector laboratories). Bound proteins were subsequently eluted from the column with N-acetyl glucosamine (Sigma-Aldrich). Equal concentrations of eluates (10 μg) were resolved by SDS-PAGE and analysed as described below.

Immunoblot analysis

Equal quantities of protein samples were resolved on 4-20% precise protein gels by SDS-PAGE (4-20% Precise Protein Gels, Thermo Fisher Scientific) and transferred to nitrocellulose membrane (Millipore). Membranes were blocked for 1 hour in 5% nonfat dry milk in TBS with 0.2% Tween 20 and incubate in primary antibodies overnight at 4 °C. Incubations were performed with the following primary antibodies: dystrophin (MANDYS1; 1:5), utrophin (MANCHO3; 1:50), α-DG IIH6 (sc-53987; 1:500; Santa Cruz Biotechnology, Inc.), β-DG (MANDAG2; 1:250), α-SG (VP-A105; 1:100), β-SG (VP-B206; 1:100), γ-SG (VP-G803; 1:100), nNOS (A-11, 1:250; Santa Cruz), laminin (L9393; 1:5,000), β1D integrin (MAB1900; 1:100), GAPDH (MAB374, 1:50,000; Chemicon) and SSPN (E2; 1:500; Santa Cruz). Horseradish peroxidase–conjugated anti–rabbit IgG and anti–mouse IgG (GE Healthcare) secondary antibodies were used at 1:2,000 dilutions in 5% nonfat dry milk and incubated at RT for 3 h. Immunoblots were developed using enhanced chemiluminescence (SuperSignal West Pico Chemiluminescent Substrate; Thermo Fisher Scientific). Mean integrated density value was quantified using ImageJ (NIH).

Laminin overlay assay

Membranes were prepared as described in sWGA enrichment of protein lysates. Membranes were blocked with 5% BSA in laminin-binding buffer (10 mM triethanolamine, 140 mM NaCl, 1 mM $MgCl_2$, and 1 mM $CaCl_2$, pH 7.6) followed by incubation of Engelbreth-Holm-Swarm laminin (354239; BD) in laminin-binding buffer for 8 h at 4 °C. Membranes were washed and incubated with rabbit anti-laminin antibody (L9393; 1:5,000; Sigma-Aldrich) overnight at 4 °C. Blots were probed with secondary and developed as described above.

Immunohistochemistry

Muscles were mounted in OCT (Tissue-Tek) and flash frozen in liquid nitrogen–cooled isopentane, and stored at − 80 °C until further processing. Transverse 7-μm transverse cryosections were blocked with 3% BSA in PBS for 30 min at room temperature. Avidin/biotin blocking kit (Vector Laboratories) was used according to manufacturer's instructions. For antibodies raised in mouse, Mouse on Mouse blocking reagent (Vector

Laboratories) was used according to manufacturer's instructions. Sections were incubated in primary antibody in PBS at 4 °C overnight with the following antibodies: dystrophin (MANDYS1; 1:5; Development Studies Hybridoma Bank), utrophin (DRP, 1:100), β-DG (MANDAG2; 1:50; Development Studies Hybridoma Bank), α-SG (VP-A105; 1:30; Vector Laboratories), β-SG (VP-B206; 1:30; Vector Laboratories), α7 integrin (C-20; 1:100; Santa Cruz), nNOS (A-11, 1:250; Santa Cruz), laminin (L9393; 1:500; Sigma-Aldrich), β1D integrin (MAB1900; 1:20; Millipore), and SSPN (E2; 1:100). Primary antibodies were detected by biotinylated anti–rabbit (BA-1000; 1:500; Vector Laboratories) and biotinylated anti–mouse (BA-9200; 1:500; Vector Laboratories). Fluorescein–conjugated avidin D (A-2001; 1:500; Vector Laboratories) was used to detect secondary antibodies and biotinylated WFA. All sections were mounted in Vectashield (Vector Laboratories) and visualized using an Axioplan 2 fluorescence microscope with Axiovision 3.0 software (Carl Zeiss Inc, Thornwood, NY, USA).

Histology

To assess general muscle pathology, transverse sections from the quadriceps, tibialis anterior, EDL, heart, intercostal, abdominal and diaphragm muscles (8 μm) were stained with H&E as described previously (16). The percentage of centrally nucleated fibres was assessed for quadriceps and diaphragm muscle from 6-week-old animals.

Evans blue dye assay

Evans blue dye (EBD) was diluted in PBS to a final concentration of 10 mg/ml and was sterilized by filtration using a 0.2 μm filter. EBD was administered by intraperitoneal injection 10-12 hours before dissection (50 μl of diluted EBD per 10 g of body weight). Quadriceps and diaphragms were processed as described above, counterstained with antibody against laminin, and visualized using fluorescence microscopy. The percentage of EBD-positive fibres was obtained by counting the number of EBD-positive fibres in a quadriceps or diaphragm section and dividing by the total number of myofibres.

Grip strength test

Forelimb grip strength was measured using a digital force gauge (Columbus Instruments, Columbus, OH). In each trial, the mouse grasped the pull bar connected to the grip strength meter and was gently pulled back until the pull bar was released. This procedure was repeated five times per trial and peak tension (N) was recorded for each trial. Five trials were performed with 1 min of rest between each trial. Fifth trial peak tension values normalized to body weight (N/g) are reported.

Open field activity

Post-exercise ambulation in 6-month-old animals was recorded immediately following grip strength testing. Mice were placed in individual recording chambers and allowed to roam freely for 6 minutes. The distance travelled by each animal was determined using frame-by-frame object tracking in Kinovea open source video analysis software (Version 0.8.15, http://www.kinovea.org; date last accessed October 21, 2016).

Serum creatine kinase assay

Blood was collected from the retro-orbital sinus of 6-month-old WT, *mdx* and *mdx*:mSSPN-Tg mice. Total serum creatine kinase (CK) levels were measured with a Beckman Coulter UV spectrometer (Fullerton, CA) using a creatine kinase reagent (CK-NAC; Teco diagnostics, Anaheim, CA) according to the manufacturer's instructions.

Mouse muscle physiology

The contractile properties of the EDL were measured as described previously by the muscle phenotyping core facility at the University of Pennsylvania (Dr. Elisabeth R. Barton, University of Pennsylvania, Philadelphia, PA) (16). Muscles were dissected, removed and placed in a bath of Ringer's solution gas-equilibrated with 95% O_2/5% CO_2. Muscles were subjected to isolated mechanical measurements. After determining the optimum length (Lo) by supramaximal twitch stimulation, maximum isometric tetanus was measured. Muscles were then subjected to a series of five eccentric contractions with a 5 min rest between contractions.

Whole body plethysmography

Pulmonary function was measured as previously described (36). Briefly, respiration was monitored in conscious, unrestrained mice using a whole body plethysmography apparatus (Buxco Research Systems). Mice were acclimatized in monitoring chambers for 1 hour at room air conditions (RA). Baseline measurements were recorded during the final 5 min of acclimatization. The mice were then exposed to hypercapnic conditions (8% CO_2/21% O_2/balance N_2) and then returned to RA for 10 min. Following RA conditions, mice were exposed to a second hypercapnic challenge. Data from the first hypercapnic challenge are included in Fig. 5; all pulmonary measurements are reported in Supplementary Materials, Tables S1 and S2.

Supplementary Material

Supplementary Material is available at HMG online.

Acknowledgements

The authors thank L. Martinez and D. Becerra for pulmonary function measurements; and Dr. E.R. Barton, Dr. M. Liu and the Paul Wellstone Muscular Dystrophy Cooperative Research Center of the National Institutes of Health [U54 AR052646] for *in vitro* physiological measurements.

Conflict of Interest statement. None declared.

Funding

This work was supported by grants from the National Institutes of Health [R01 AR048179 to R.C.W, T32 GM07104 to J.L.M., T32 AR059033 to J.L.M. and E.M.G]; the UCLA Center for Duchenne Muscular Dystrophy Mouse Phenotyping and Imaging Core [P30 AR057230]; the UCLA Clinical and Translational Science Institute (UL1TR000124); the Edith Hyde Fellowship [to J.L.M.]; the Eureka Pre-doctoral Training Fellowship [to J.L.M.]; the UCLA Undergraduate Research Scholars Program [to E.M.] and the Muscular Dystrophy Association USA [274143 to R.C.W.]. Funding to pay the Open Access publication charges for this

article was provided by the NIH (R01 AR048179 to R.C.W, "Structure-Function Analysis of Sarcospan").

References

1. Hoffman, E.P., Brown, R.H. and Kunkel, L.M. (1987) Dystrophin: the protein product of the Duchenne muscular dystrophy locus. *Cell*, **51**, 919–928.
2. Bonilla, E., Samitt, C.E., Miranda, A.F., Hays, A.P., Salviati, G., DiMauro, S., Kunkel, L.M., Hoffman, E.P. and Rowland, L.P. (1988) Duchenne muscular dystrophy: deficiency of dystrophin at the muscle cell surface. *Cell*, **54**, 447–452.
3. Campbell, K.P. and Kahl, S.D. (1989) Association of dystrophin and an integral membrane glycoprotein. *Nature*, **338**, 259–262.
4. Ibraghimov-Beskrovnaya, O., Ervasti, J.M., Leveille, C.J., Slaughter, C.A., Sernett, S.W. and Campbell, K.P. (1992) Primary structure of dystrophin-associated glycoproteins linking dystrophin to the extracellular matrix. *Nature*, **355**, 696–702.
5. Ervasti, J.M. and Campbell, K.P. (1993) A role for the dystrophin-glycoprotein complex as a transmembrane linker between laminin and actin. *J. Cell Biol.*, **122**, 809–823.
6. Yoshida, M. and Ozawa, E. (1990) Glycoprotein complex anchoring dystrophin to sarcolemma. *J. Biochem.*, **108**, 748–752.
7. Petrof, B.J., Shrager, J.B., Stedman, H.H., Kelly, A.M. and Sweeney, H.L. (1993) Dystrophin protects the sarcolemma from stresses developed during muscle contraction. *Proc. Natl. Acad. Sci. USA*, **90**, 3710–3714.
8. Weller, B., Karpati, G. and Carpenter, S. (1990) Dystrophin-deficient mdx muscle fibers are preferentially vulnerable to necrosis induced by experimental lengthening contractions. *J. Neurol. Sci.*, **100**, 9–13.
9. Tinsley, J.M., Blake, D.J., Roche, A., Fairbrother, U., Riss, J., Byth, B.C., Knight, A.E., Kendrick-Jones, J., Suthers, G.K., Love, D.R., *et al.* (1992) Primary structure of dystrophin-related protein. *Nature*, **360**, 591–593.
10. von der Mark, H., Durr, J., Sonnenberg, A., von der Mark, K., Deutzmann, R. and Goodman, S.L. (1991) Skeletal myoblasts utilize a novel beta 1-series integrin and not alpha 6 beta 1 for binding to the E8 and T8 fragments of laminin. *J. Biol. Chem.*, **266**, 23593–23601.
11. Song, W.K., Wang, W., Foster, R.F., Bielser, D.A. and Kaufman, S.J. (1992) H36-alpha 7 is a novel integrin alpha chain that is developmentally regulated during skeletal myogenesis. *J. Cell Biol.*, **117**, 643–657.
12. Pearce, M., Blake, D.J., Tinsley, J.M., Byth, B.C., Campbell, L., Monaco, A.P. and Davies, K.E. (1993) The utrophin and dystrophin genes share similarities in genomic structure. *Hum. Mol. Genet.*, **2**, 1765–1772.
13. Matsumura, K., Ervasti, J.M., Ohlendieck, K., Kahl, S.D. and Campbell, K.P. (1992) Association of dystrophin-related protein with dystrophin-associated proteins in mdx mouse muscle. *Nature*, **360**, 588–591.
14. Crosbie, R.H., Heighway, J., Venzke, D.P., Lee, J.C. and Campbell, K.P. (1997) Sarcospan: the 25kDa transmembrane component of the dystrophin-glycoprotein complex. *J. Biol. Chem.*, **272**, 31221–31224.
15. Crosbie, R.H., Lebakken, C.S., Holt, K.H., Venzke, D.P., Straub, V., Lee, J.C., Grady, R.M., Chamberlain, J.S., Sanes, J.R. and Campbell, K.P. (1999) Membrane targeting and stabilization of sarcospan is mediated by the sarcoglycan subcomplex. *J. Cell Biol.*, **145**, 153–165.
16. Marshall, J.L., Chou, E., Oh, J., Kwok, A., Burkin, D.J. and Crosbie-Watson, R.H. (2012) Dystrophin and utrophin expression require sarcospan: loss of alpha7 integrin exacerbates a newly discovered muscle phenotype in sarcospan-null mice. *Hum. Mol. Genet.*, **21**, 4378–4393.
17. Marshall, J.L., Oh, J., Chou, E., Lee, J.A., Holmberg, J., Burkin, D.J. and Crosbie-Watson, R.H. (2015) Sarcospan integration into laminin-binding adhesion complexes that ameliorate muscular dystrophy requires utrophin and alpha7 integrin. *Hum. Mol. Genet.*, **24**, 2011–2022.
18. Peter, A.K., Marshall, J.L. and Crosbie, R.H. (2008) Sarcospan reduces dystrophic pathology: stabilization of the utrophin-glycoprotein complex. *J. Cell Biol.*, **183**, 419–427.
19. Marshall, J.L., Holmberg, J., Chou, E., Ocampo, A.C., Oh, J., Lee, J., Peter, A.K., Martin, P.T. and Crosbie-Watson, R.H. (2012) Sarcospan-dependent Akt activation is required for utrophin expression and muscle regeneration. *J. Cell Biol.*, **197**, 1009–1027.
20. Marshall, J.L., Kwok, Y., McMorran, B.J., Baum, L.G. and Crosbie-Watson, R.H. (2013) The potential of sarcospan in adhesion complex replacement therapeutics for the treatment of muscular dystrophy. *Febs J.*, **280**, 4210–4229.
21. Rafael, J.A., Tinsley, J.M., Potter, A.C., Deconinck, A.E. and Davies, K.E. (1998) Skeletal muscle-specific expression of a utrophin transgene rescues utrophin-dystrophin deficient mice. *Nat. Genet.*, **19**, 79–82.
22. Tinsley, J., Deconinck, N., Fisher, R., Kahn, D., Phelps, S., Gillis, J.M. and Davies, K. (1998) Expression of full-length utrophin prevents muscular dystrophy in mdx mice. *Nat. Med.*, **4**, 1441–1444.
23. Gilbert, R., Nalbantoglu, J., Petrof, B.J., Ebihara, S., Guibinga, G.H., Tinsley, J.M., Kamen, A., Massie, B., Davies, K.E. and Karpati, G. (1999) Adenovirus-mediated utrophin gene transfer mitigates the dystrophic phenotype of mdx mouse muscles. *Hum. Gene Ther.*, **10**, 1299–1310.
24. Fisher, R., Tinsley, J.M., Phelps, S.R., Squire, S.E., Townsend, E.R., Martin, J.E. and Davies, K.E. (2001) Non-toxic ubiquitous over-expression of utrophin in the mdx mouse. *Neuromuscul. Disord.*, **11**, 713–721.
25. Burkin, D.J., Wallace, G.Q., Milner, D.J., Chaney, E.J., Mulligan, J.A. and Kaufman, S.J. (2005) Transgenic expression of {alpha}7{beta}1 integrin maintains muscle integrity, increases regenerative capacity, promotes hypertrophy, and reduces cardiomyopathy in dystrophic mice. *Am. J. Pathol.*, **166**, 253–263.
26. Parvatiyar, M.S., Marshall, J.L., Nguyen, R.T., Jordan, M.C., Richardson, V.A., Roos, K.P. and Crosbie-Watson, R.H. (2015) Sarcospan Regulates Cardiac Isoproterenol Response and Prevents Duchenne Muscular Dystrophy-Associated Cardiomyopathy. *J. Am. Heart Assoc.*, **4**: e002481.
27. Peter, A.K., Miller, G. and Crosbie, R.H. (2007) Disrupted mechanical stability of the dystrophin-glycoprotein complex causes severe muscular dystrophy in sarcospan transgenic mice. *J. Cell Sci.*, **120**, 996–1008.
28. Straub, V., Rafael, J.A., Chamberlain, J.S. and Campbell, K.P. (1997) Animal models for muscular dystrophy show different patterns of sarcolemmal disruption. *J. Cell Biol.*, **139**, 375–385.
29. Brenman, J.E., Chao, D.S., Xia, H., Aldape, K. and Bredt, D.S. (1995) Nitric oxide synthase complexed with dystrophin and absent from skeletal muscle sarcolemma in Duchenne muscular dystrophy. *Cell*, **82**, 743–752.
30. Kobayashi, Y.M., Rader, E.P., Crawford, R.W., Iyengar, N.K., Thedens, D.R., Faulkner, J.A., Parikh, S.V., Weiss, R.M.,

Chamberlain, J.S., Moore, S.A., *et al.* (2008) Sarcolemma-localized nNOS is required to maintain activity after mild exercise. *Nature*, **456**, 511–515.
31. Sander, M., Chavoshan, B., Harris, S.A., Iannaccone, S.T., Stull, J.T., Thomas, G.D. and Victor, R.G. (2000) Functional muscle ischemia in neuronal nitric oxide synthase-deficient skeletal muscle of children with Duchenne muscular dystrophy. *Proc. Natl Acad. Sci. U S A*, **97**, 13818–13823.
32. Stedman, H.H., Sweeney, H.L., Shrager, J.B., Maguire, H.C., Panettieri, R.A., Petrof, B., Narusawa, M., Leferovich, J.M., Sladky, J.T. and Kelly, A.M. (1991) The mdx mouse diaphragm reproduces the degenerative changes of Duchenne muscular dystrophy. *Nature*, **352**, 536–539.
33. Ishizaki, M., Suga, T., Kimura, E., Shiota, T., Kawano, R., Uchida, Y., Uchino, K., Yamashita, S., Maeda, Y.,. and Uchino, M. (2008) Mdx respiratory impairment following fibrosis of the diaphragm. *Neuromuscul. Disord.*, **18**, 342–348.
34. Gao, Q.Q., Wyatt, E., Goldstein, J.A., LoPresti, P., Castillo, L.M., Gazda, A., Petrossian, N., Earley, J.U., Hadhazy, M., Barefield, D.Y., *et al.* (2015) Reengineering a transmembrane protein to treat muscular dystrophy using exon skipping. *J. Clin. Invest.*, **125**, 4186–4195.
35. Tangsrud, S., Petersen, I.L., Lodrup Carlsen, K.C. and Carlsen, K.H. (2001) Lung function in children with Duchenne's muscular dystrophy. *Respir. Med.*, **95**, 898–903.
36. Capote, J., Kramerova, I., Martinez, L., Vetrone, S., Barton, E.R., Sweeney, H.L., Miceli, M.C. and Spencer, M.J. (2016) Osteopontin ablation ameliorates muscular dystrophy by shifting macrophages to a pro-regenerative phenotype. *J. Cell Biol.*, **213**, 275–288.
37. Lebakken, C.S., Venzke, D.P., Hrstka, R.F., Consolino, C.M., Faulkner, J.A., Williamson, R.A. and Campbell, K.P. (2000) Sarcospan-deficient mice maintain normal muscle function. *Mol. Cell. Biol.*, **20**, 1669–1677.
38. Moorwood, C., Liu, M., Tian, Z. and Barton, E.R. (2013) Isometric and eccentric force generation assessment of skeletal muscles isolated from murine models of muscular dystrophies. *J. Vis. Exp.*, e50036.
39. Kobayashi, Y.M., Rader, E.P., Crawford, R.W. and Campbell, K.P. (2012) Endpoint measures in the mdx mouse relevant for muscular dystrophy pre-clinical studies. *Neuromuscul. Disord.*, **22**, 34–42.
40. Gosselin, L.E., Barkley, J.E., Spencer, M.J., McCormick, K.M. and Farkas, G.A. (2003) Ventilatory dysfunction in mdx mice: impact of tumor necrosis factor-alpha deletion. *Muscle Nerve*, **28**, 336–343.
41. Burns, D.P., Edge, D., O'Malley, D. and O'Halloran, K.D. (2015) Respiratory Control in the mdx Mouse Model of Duchenne Muscular Dystrophy. *Adv. Exp. Med. Biol.*, **860**, 239–244.
42. Hoffman, E.P. and McNally, E.M. (2014) Exon-skipping therapy: a roadblock, detour, or bump in the road?. *Sci. Transl. Med.*, **6**, 230fs214.
43. Crawford, G.E., Faulkner, J.A., Crosbie, R.H., Campbell, K.P., Froehner, S.C. and Chamberlain, J.S. (2000) Assembly of the dystrophin-associated protein complex does not require the dystrophin COOH-terminal domain. *J. Cell Biol.*, **150**, 1399–1410.